

LA-UR-16-28568

Approved for public release; distribution is unlimited.

Title: Semi-Analytical Benchmarks for MCNP6

Author(s): Grechanuk, Pavel Aleksandrovi

Intended for: Report

Issued: 2016-11-07

Disclaimer:

Los Alamos National Laboratory, an affirmative action/equal opportunity employer, is operated by the Los Alamos National Security, LLC for the National Nuclear Security Administration of the U.S. Department of Energy under contract DE-AC52-06NA25396. By approving this article, the publisher recognizes that the U.S. Government retains nonexclusive, royalty-free license to publish or reproduce the published form of this contribution, or to allow others to do so, for U.S. Government purposes. Los Alamos National Laboratory requests that the publisher identify this article as work performed under the auspices of the U.S. Department of Energy. Los Alamos National Laboratory strongly supports academic freedom and a researcher's right to publish; as an institution, however, the Laboratory does not endorse the viewpoint of a publication or guarantee its technical correctness.

Semi-Analytical Benchmarks for MCNP6

Pavel Grechanuk

September 15, 2016

1 Introduction

Code verification is an extremely important process that involves proving or disproving the validity of code algorithms by comparing them against analytical results of the underlying physics or mathematical theory on which the code is based upon. Monte Carlo codes such as MCNP6 must undergo verification and testing upon every release to ensure that the codes are properly simulating nature [2]. Specifically, MCNP6 has multiple sets of problems with known analytic solutions that are used for code verification. Most of the verification problems are fairly simple due to the fact that they are usually composed of few materials, with simplified cross-sections, and simple geometry. The simplicity makes the problems easily solvable mathematically, and thus they are quite valuable in verifying that the code algorithms and methods are operating as intended.

1.1 Benchmarks

Most of the analytical benchmarks for fixed source transport problems used for code verification specify either the boundary conditions for the angular or scalar flux or the external (usually isotropic) source. Monte Carlo codes on the other hand, primarily specify either current boundary sources or a volumetric fixed source, either of which can be very complicated functions of space, energy, direction and time. Thus, most of the challenges with modeling analytic benchmark problems in Monte Carlo codes come from identifying the correct source definition to properly simulate the correct boundary conditions. In this benchmark suite, the problems included originate from chapter 3 of Barry Ganapol's book, *Analytical Benchmarks for Nuclear Engineering Applications – Case Studies in Neutron Transport Theory* [1].

1.2 Theory

The problems included in this suite all deal with mono-energetic neutron transport without energy loss, in a homogeneous material. The variables that differ between the problems are source type

(isotropic/beam), medium dimensionality (infinite/semi-infinite), and c (defined below).

$$c \equiv \frac{\Sigma_s + \nu\Sigma_f}{\Sigma_t} \quad (1)$$

For all of these benchmarks, while the ratio of c is varied, Σ_t is always kept at unity. The mono-energetic approximation allows the benchmark problems to be solved analytically. To get to the one group form, we assume neutrons scatter elastically from nuclei with infinite mass and thus do not lose energy. After integrating out energy we obtain the one group version of the transport equation:

$$[\Omega \cdot \Delta + \Sigma(r, E_0)] \phi(r, \Omega) = \int_{4\pi} d\Omega' \Sigma_s(r, \Omega' \cdot \Omega, E_0) \phi(r, \Omega') + \frac{1}{4\pi} \nu(E_0) \Sigma_f(r, E_0) \int_{4\pi} d\Omega' \phi(r, \Omega') + Q(r, \Omega) \quad (2)$$

Equation (2) has three dimensions and thus is still difficult to solve mathematically. Further simplifications are necessary in order to be able to reach a solution analytically, like a reduction to 1-D geometry, and cross-sections which only include elastic scatter, capture and fission neutron physics.

2 Results

Professor Ganapol provided the FORTRAN codes that were used to solve modified versions of the mono-energetic transport equation semi-analytically, for the different boundary conditions and values of c . The same problems were set up in MCNP6, and the data was compared using a python script. For ease of comparison, the numbering of the plots coincide with the numbering in Barry Ganapol's book [1].

2.1 Benchmark 3.1

For Benchmark 3.1 the transport equation that is solved is for mono-energetic neutrons in a homogeneous infinite medium, scattering without energy loss:

$$\left[\mu \frac{\partial}{\partial x} + \Sigma \right] \phi(x, \mu) = \frac{1}{2} \sum_{l=0}^{\infty} (2l+1) \Sigma_{sl} P_l(\mu) \phi_l(x) + \frac{1}{2} \nu \Sigma_f \phi_0(x) + Q(x, \mu) \quad (3)$$

With some mathematical manipulation this equation can be solved for either a beam or isotropic source at the center of an infinite medium. By measuring the spatial variable in mean free paths, and combining scattering and fission the following equation is obtained:

$$\left[\mu \frac{\partial}{\partial x} + 1 \right] \phi(x, \mu) = \frac{1}{2} c_s \sum_{l=0}^{\infty} (2l+1) f_{sl} P_l(\mu) \phi_l(x) + \frac{1}{2} c_f \phi_0(x) + Q(x, \mu) \quad (4)$$

For this group of problems the source is defined as either:

$$Q(\mu) \equiv \begin{cases} 1/2, & \text{Isotropic} \\ \delta(\mu - \mu_0), & \text{Beam} \end{cases} \quad (5)$$

2.1.1 Benchmark 3.1.1 Beam Source in an Infinite Medium

For Benchmark 3.1.1, the results from MCNP6 agree very closely with the analytic solution as can be seen in Figure (1). The figure shows results using two values of c , for a beam source at the origin of an infinite medium, with a direction of $\mu_0 = 1$ relative to the positive x direction. A F2 flux tally was used in MCNP6, and the infinite boundary was set at 100 cm from the origin in both directions. The statistical error bars from MCNP6 are too small to make out on the plot.

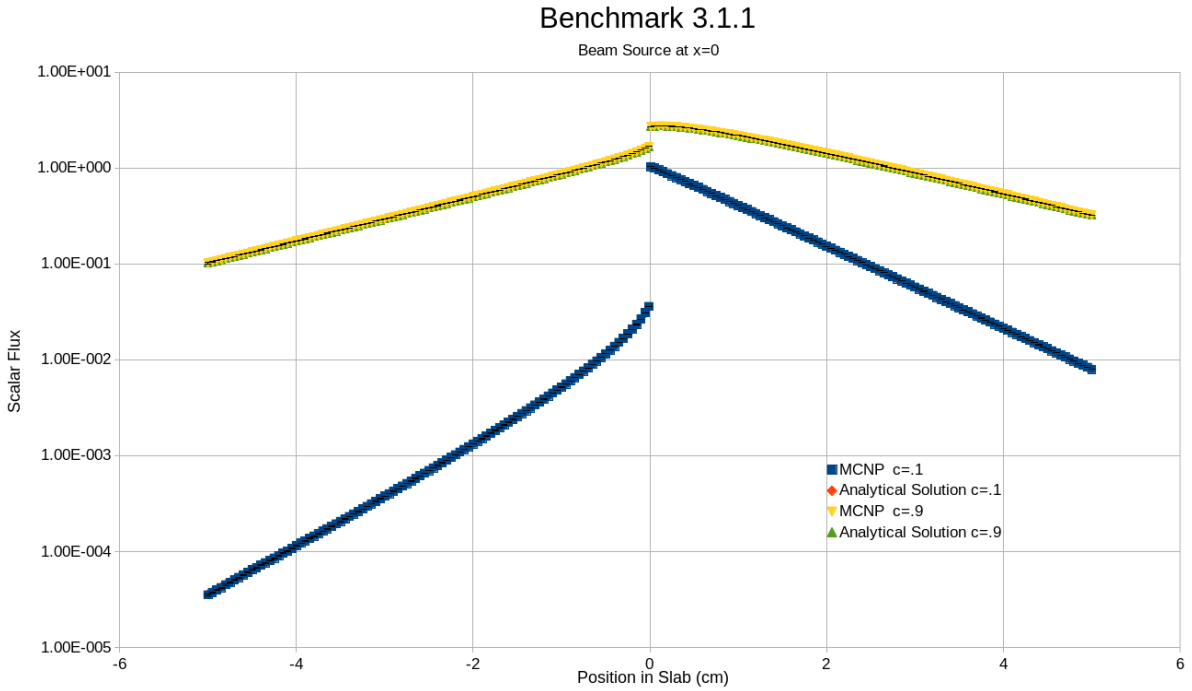


Figure 1: Comparison of analytic results for Benchmark 3.1.1 with MCNP6 results for a beam source.

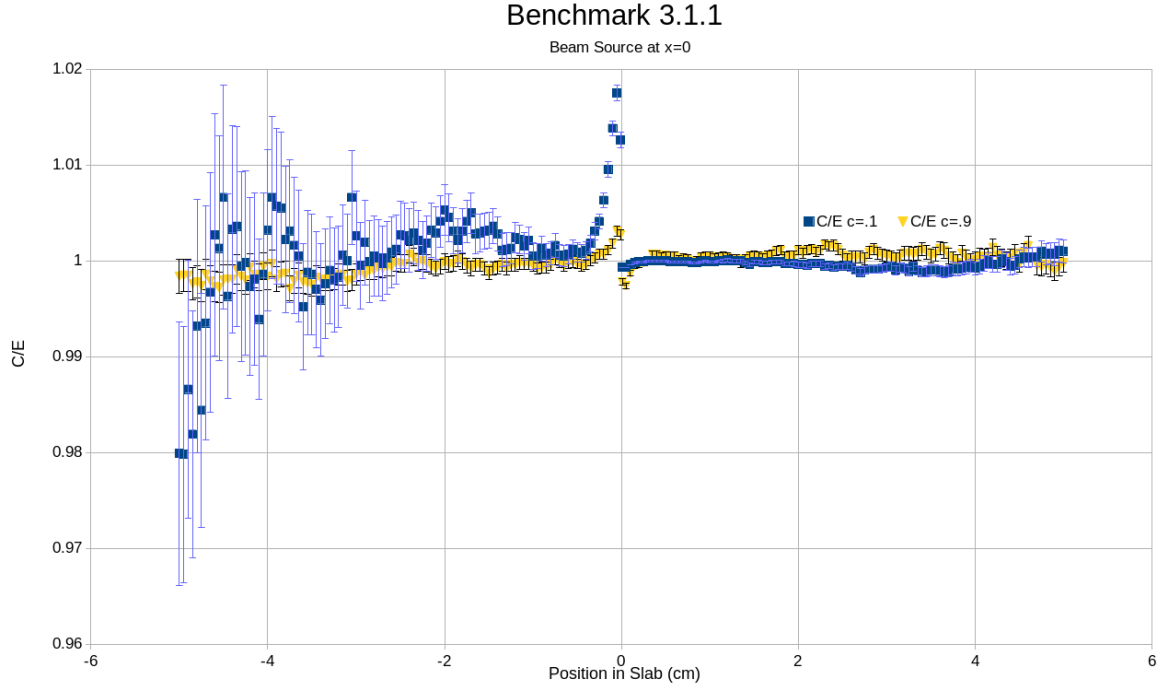


Figure 2: MCNP6 values divided by the analytic solution for Benchmark 3.1.1.

As can be seen from Figure (2), the main discrepancies occur for the high absorption system ($c=.1$). Due to the beam traveling in the positive x direction, the statistics are not as resolved in the negative region due to under-sampling. The region where the flux is least accurate can be observed as you move close to the source, this is most likely due to the way the F2 tally approximates flux when the cosine of the neutron direction crossing the surface becomes $|\mu| < .1$.

$$\phi = \frac{1}{A * W} \sum \frac{wgt}{|\mu|} \quad (6)$$

As can be seen from equation (6) the F2 flux tally divides by the absolute value of the particle grazing angle with the surface. Below $|\mu| < .1$ MCNP6 makes a constant contribution to the F2 tally, in order to ensure that the variance of the flux is finite and to maintain good statistics. This effect can be seen in most of the benchmarks included in this suite.

2.1.2 Benchmark 3.1.2 Isotropic Source in an Infinite Medium

In Benchmark 3.1.2 the beam is replaced with an isotropic source, while everything else is kept the same. Figure (3) shows the scalar flux with two values of c for an isotropic source in an infinite medium.

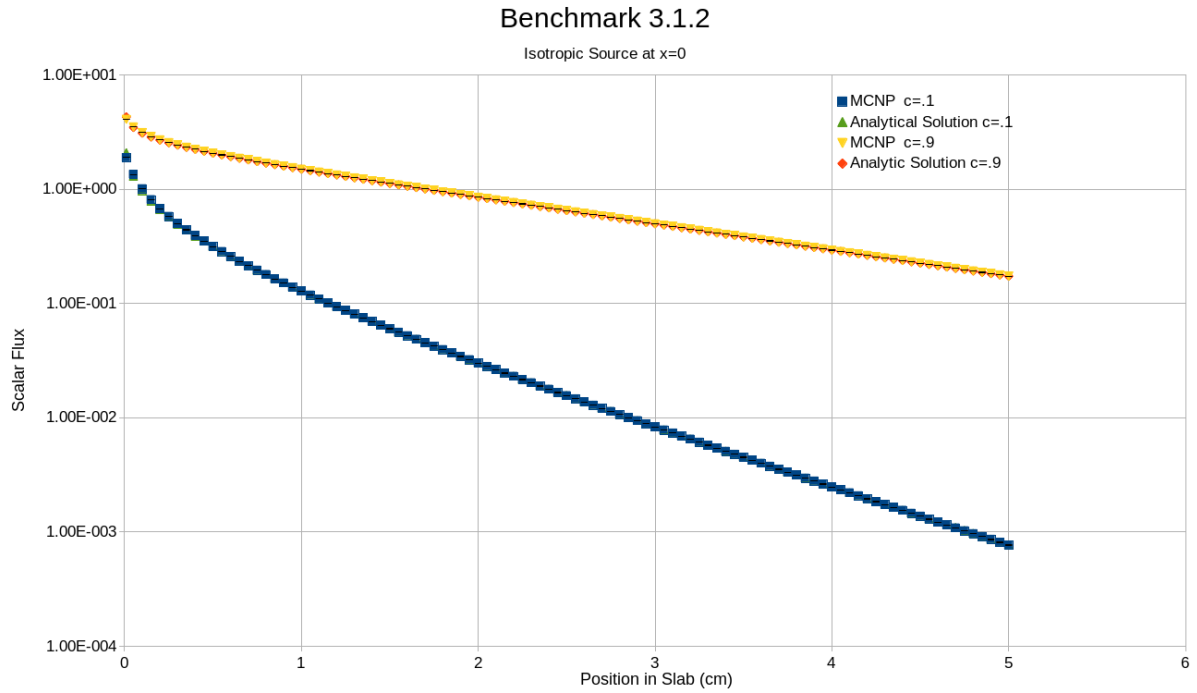


Figure 3: Comparison of analytic results for Benchmark 3.1.2 with MCNP6 results for an isotropic source.

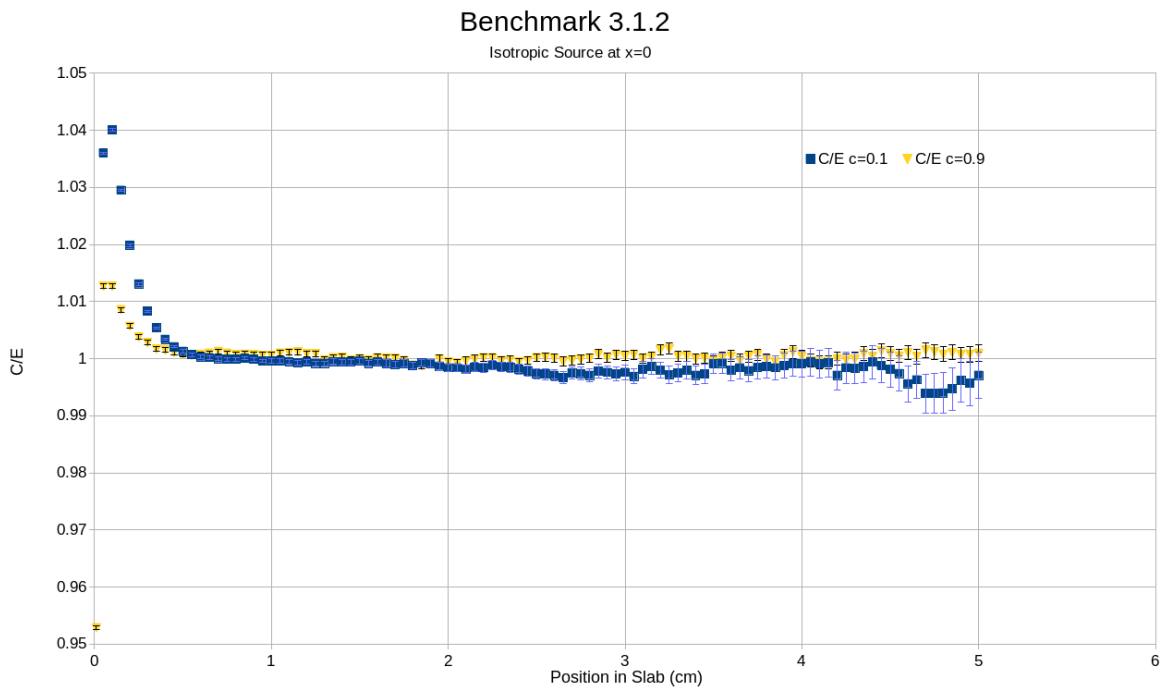


Figure 4: MCNP6 values divided by the analytic solution for Benchmark 3.1.2.

As can be seen from Figure (4) the MCNP6 results closely match the analytic solution, except close to the source where the solutions differ by as much as 4%. This is most likely due to the F2 tally, dealing with the low grazing angles coming off the isotropic source.

2.1.3 Benchmark 3.1.3 Varying Beam Angle in an Infinite Medium

Benchmark 3.1.3 has the same setup as 3.1.1 except that the angle of the beam is varied, while keeping $c=0.7$. In this case μ is measured relative to the positive x direction. By looking at Figure (5) it can be seen that the MCNP6 results closely match the analytic solution at most points. The error bars are not visible due to their small size (less than 2% of the value)

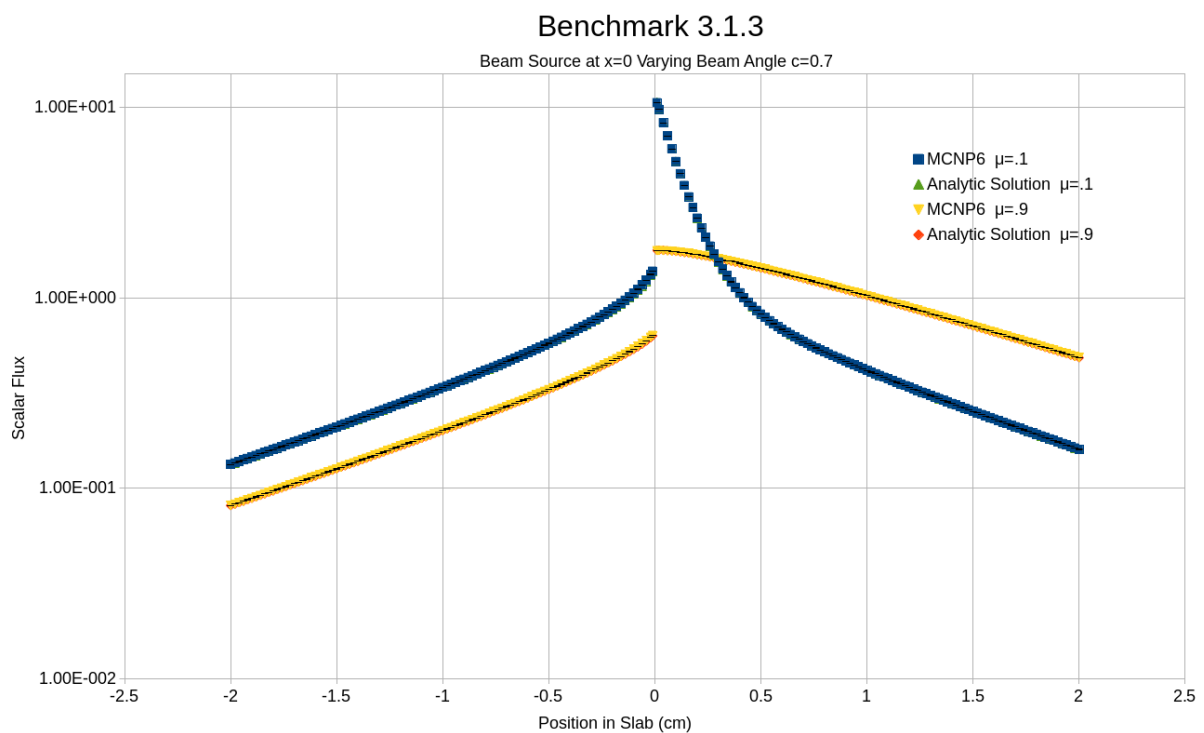


Figure 5: Comparison of analytic results for Benchmark 3.1.3 ($c=0.7$) with MCNP6 results for beam source w/varying beam angle.

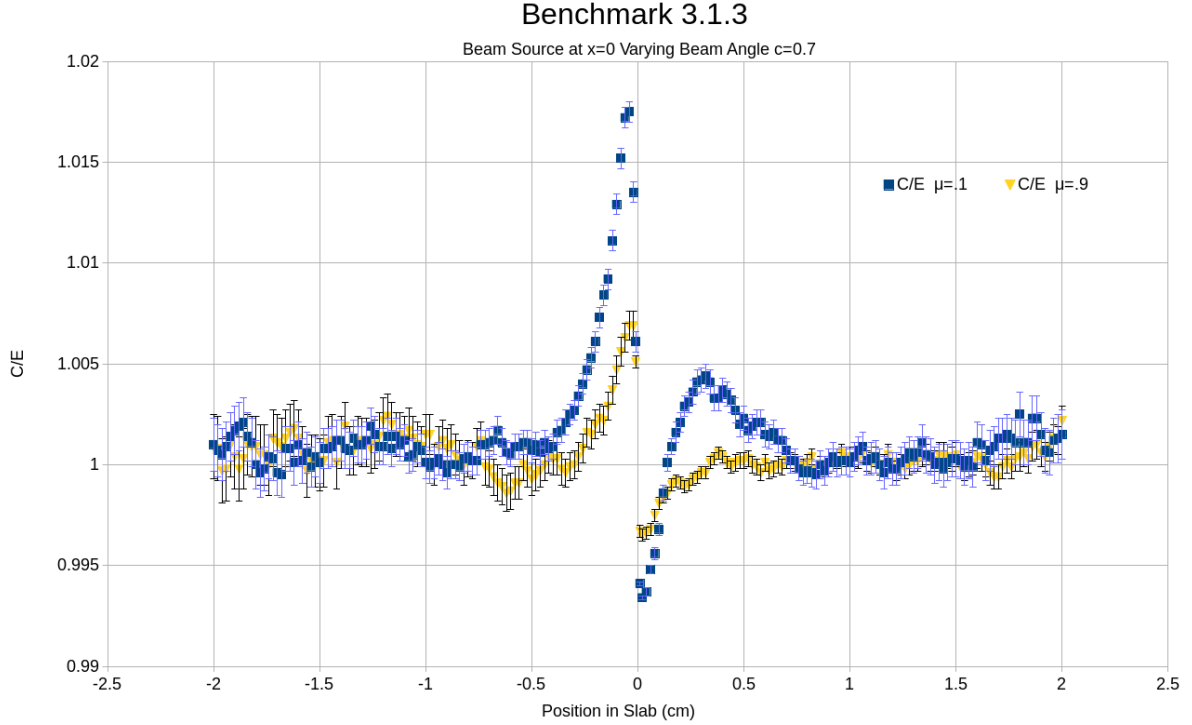


Figure 6: MCNP6 values divided by the analytic solution for Benchmark 3.1.3 ($c=0.7$).

As can be seen on Figure (6) the greatest difference between the analytic solution and MCNP6 is 1.75%, and occurs near the source, which can be explained by the F2 tally. Since the beam is no longer perpendicular to the surfaces in MCNP6, the number of particles grazing the surface with $|\mu| < .1$ is increased. It is particularly evident with the $\mu = .1$ case, as that is the cutoff point for constant contributions to the F2 tally in MCNP6.

2.2 Benchmark 3.2

For Benchmark 3.2 and 3.3 the problem to be solved is mono-energetic neutron transport through a homogeneous material with vacuum boundary conditions either on one (half space) or both sides (finite slab) and an impinging beam on the left surface. A flux F2 tally was used for these problems, and the positive infinity limit was set at 100 cm. Assuming isotropic scattering, without a distributed source, and distance measured in mean free path the transport equation to be solved is:

$$\left[\mu \frac{\partial}{\partial x} + 1 \right] \phi(x, \mu) = \frac{c}{2} \int_{-1}^1 d\mu' \phi(x, \mu') \quad (7)$$

For Benchmark 3.2 the source is defined as:

$$Q(\mu) \equiv \begin{cases} 1, & \text{Isotropic} \\ \delta(\mu - \mu_0), & \text{Beam} \end{cases} \quad (8)$$

With a boundary condition of:

$$\lim_{x \rightarrow \infty} \phi(x, \mu) < \infty \quad (9)$$

2.2.1 Benchmark 3.2.2(a) Beam Source in Half Space

In this benchmark the neutrons enter the free surface of a homogeneous semi-infinite medium. The nuclei of the material have sufficient mass to scatter the neutrons without energy loss and isotropically. As can be seen from Figure (7) and Figure (8) the analytic results match very closely to the MCNP6 results, with the greatest difference being less than 0.5%.

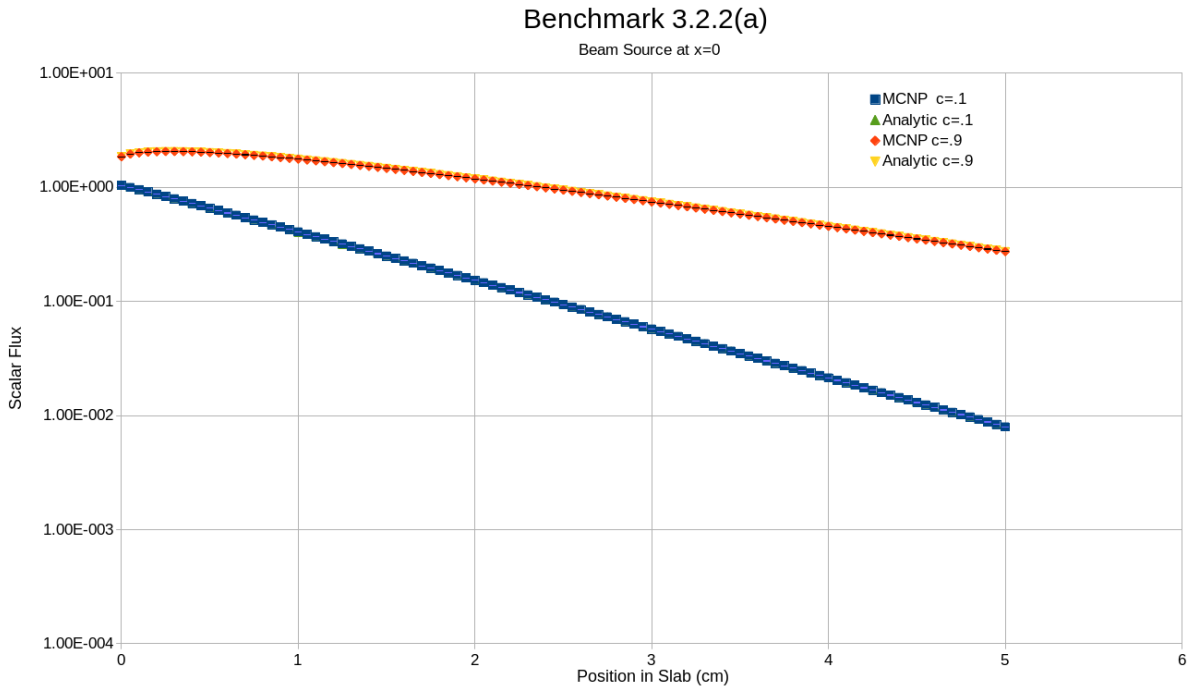


Figure 7: Comparison of analytic results for Benchmark 3.2.2(a) with MCNP6 results for beam source in half space.

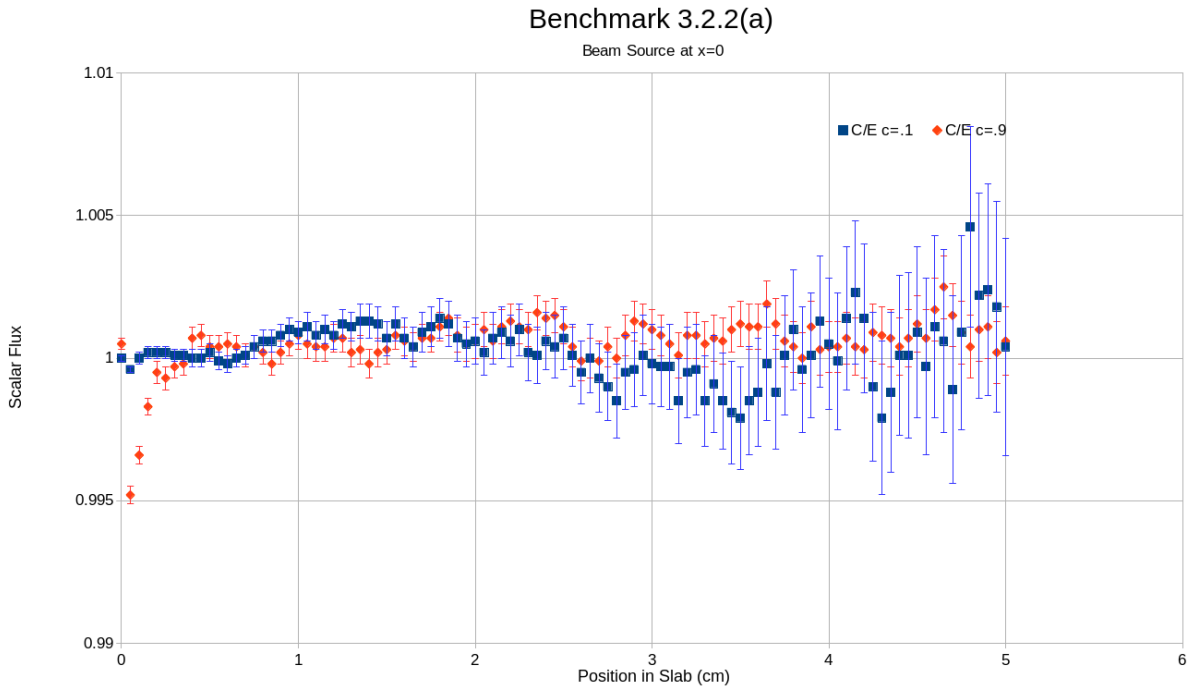


Figure 8: MCNP6 values divided by the analytic solution for Benchmark 3.2.2(a).

The F2 flux effect can again be seen for the high scattering system ($c=.9$) near the source.

2.2.2 Benchmark 3.2.2(b) Isotropic Source in Half Space

This benchmark is exactly the same as 3.2.2(a), except that the source is isotropic rather than a beam. The results can be seen in Figure (9), and again the results match very closely to the analytical solution.

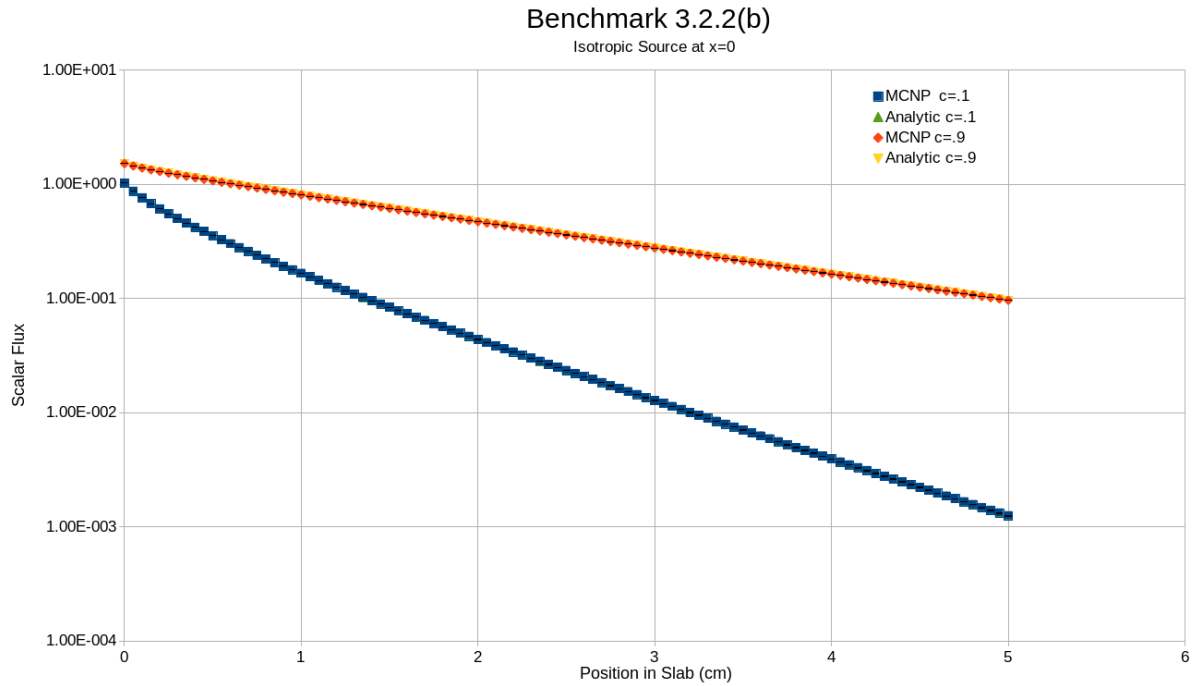


Figure 9: Comparison of analytic results for Benchmark 3.2.2(b) with MCNP6 results for an isotropic source in half space.

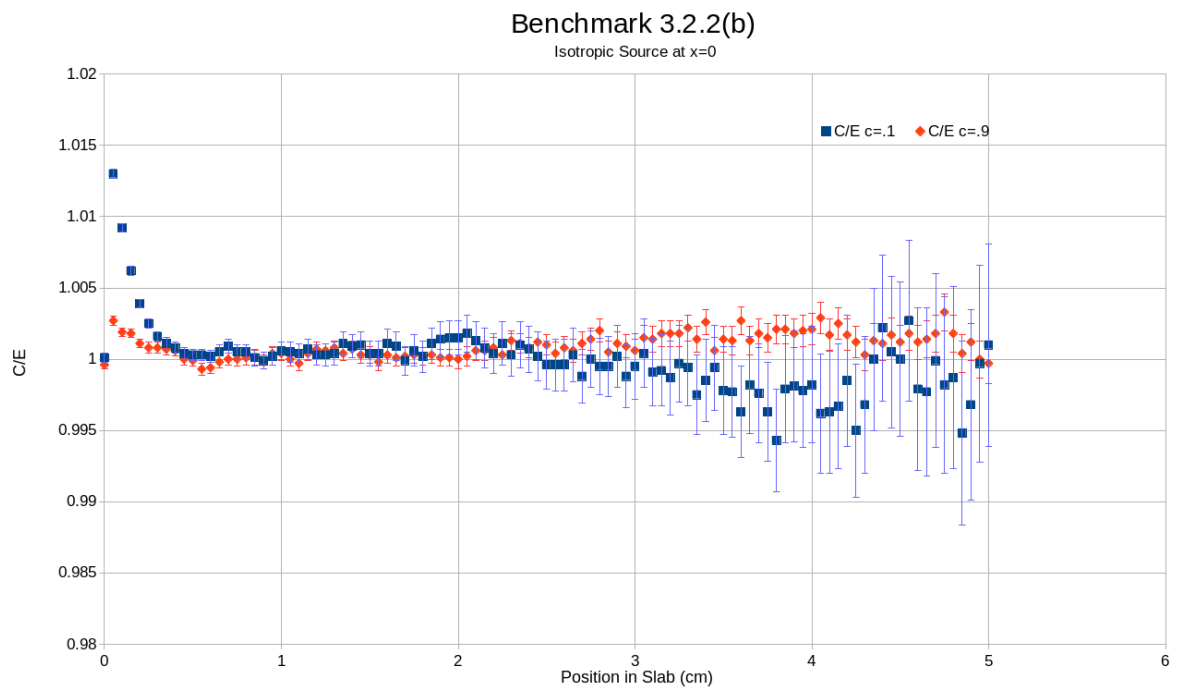


Figure 10: MCNP6 values divided by the analytic solution for Benchmark 3.2.2(b).

As can be seen from Figure (10) the F2 tally increases the flux as you approach the source, but directly at the source the MCNP6 value is correct for both cases.

2.3 Benchmark 3.3

Benchmark 3.3 solves the same exact transport equation as Benchmark 3.2, except that it is now a finite slab with vacuum boundary conditions on both sides. The following boundary conditions apply for $\mu > 0$:

$$\phi(0, \mu) = F_L(\mu) \tag{10a}$$

$$\phi(\Delta, -\mu) = 0 \tag{10b}$$

For this benchmark the material is infinite in y and z, and finite in x. The source is a beam with $\mu_0 = 1$, and it impacts a slab with varying thickness from the left. As the neutrons interact with the material, some are reflected backwards out of the slab, and a portion of neutrons make it completely through the slab and exit the other end. Given enough neutrons an angular flux distribution forms at both ends, and that is the value measured for this benchmark (divided into cosine bins between 0 and 1). This problem was set up using a (F1) current tally, while the next section solves the same problems with a (F2) flux tally.

2.3.1 Benchmark 3.3.1 Beam Source & Varying Slab Thickness (Current Tally)

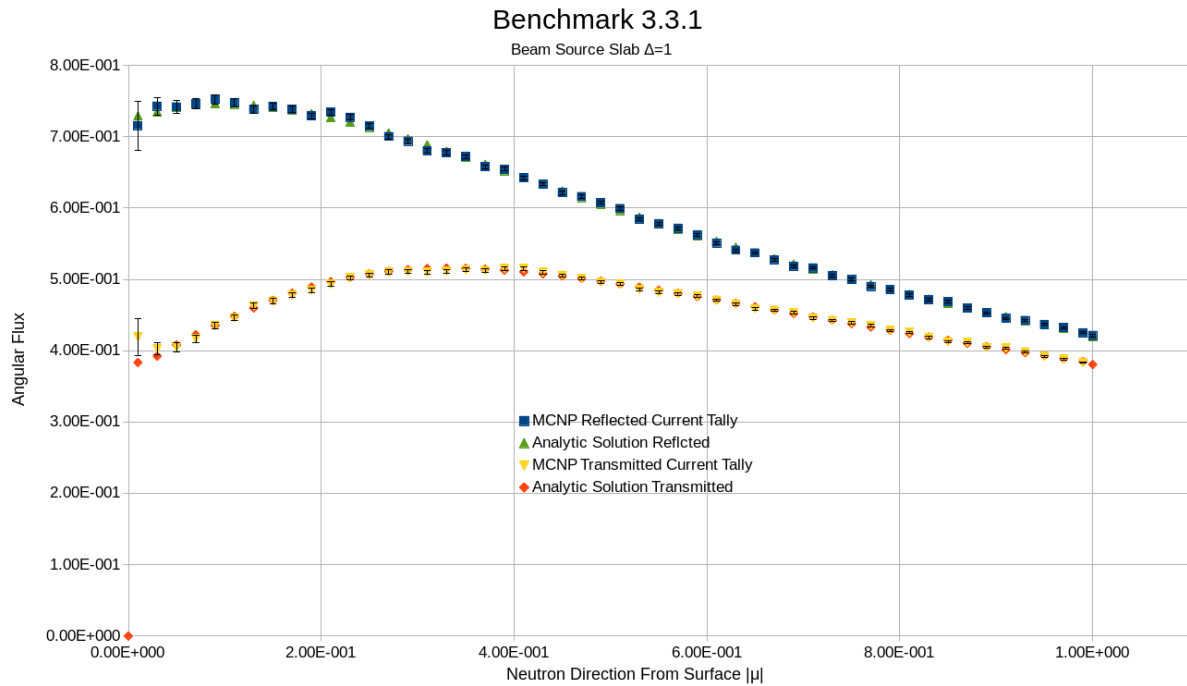


Figure 11: Comparison of analytic results for Benchmark 3.3.1 ($c=0.9$) with MCNP6 results for beam source with 1 cm slab.

For a slab thickness of 1 cm a portion of the neutrons steam through without interacting, and MCNP6 records that as a spike at $\mu = 1$ for the transmitted flux. The spike was omitted from the plots for readability purposes. The transmitted result from MCNP6 and the analytic solution diverge for the flux traveling parallel to the surface at $\mu = 0$.

Benchmark 3.3.1

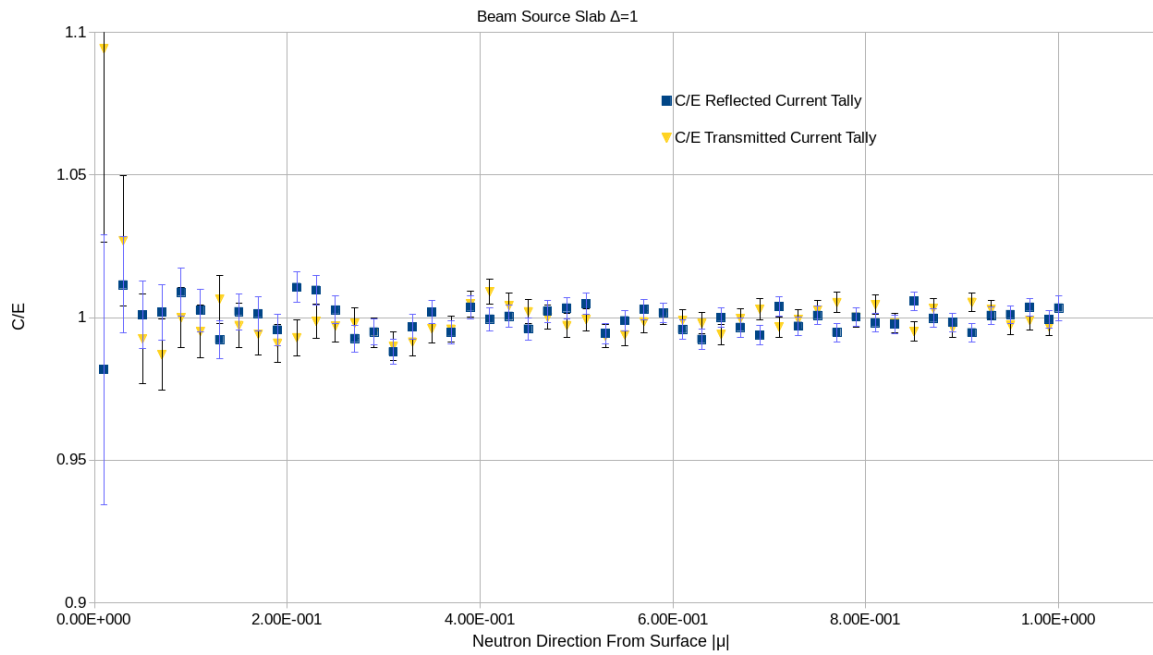


Figure 12: MCNP6 values divided by the analytic solution for Benchmark 3.3.1 ($c=0.9$) for beam source with 1 cm slab.

As can be seen from Figure (12) most of the reflected and transmitted results match closely to the analytic solution.

Benchmark 3.3.1

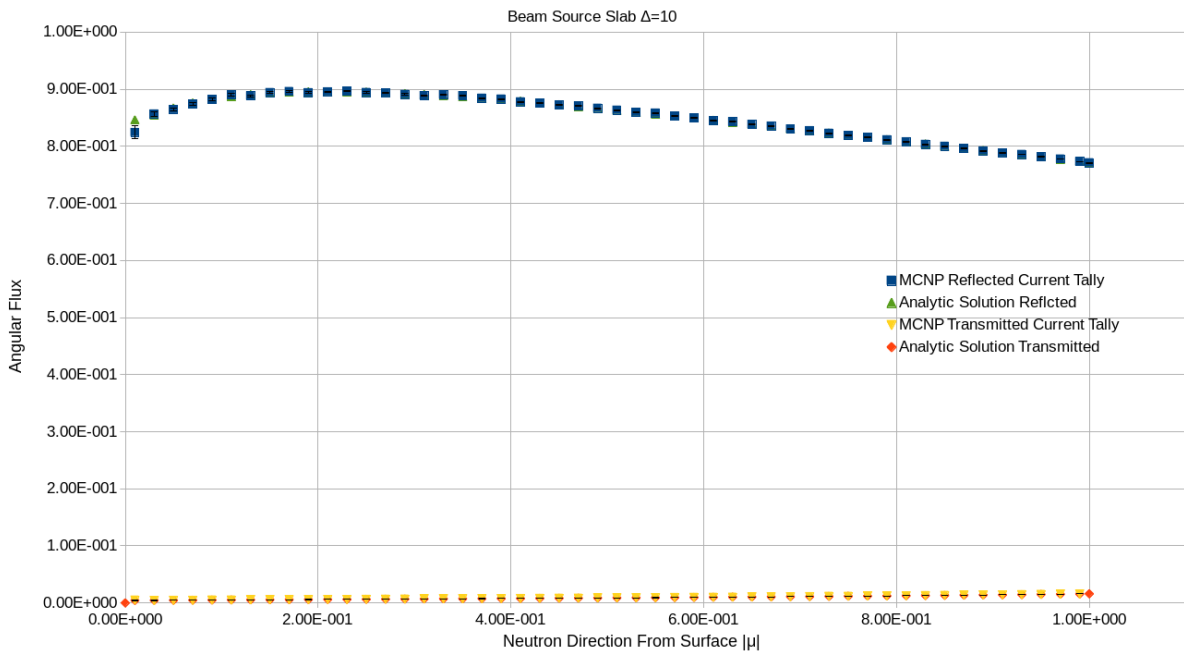


Figure 13: Comparison of analytic results for Benchmark 3.3.1 ($c=0.9$) with MCNP6 results for beam source with 10 cm slab.

In Figure (13) and Figure (14) the slab width is 10 cm, and there is greater variance on the transmitted flux, most likely because the far region is under-sampled. The MCNP6 values for the reflected flux match closely to the analytic solution, with the greatest error occurring at the $\mu = 0$ bin.

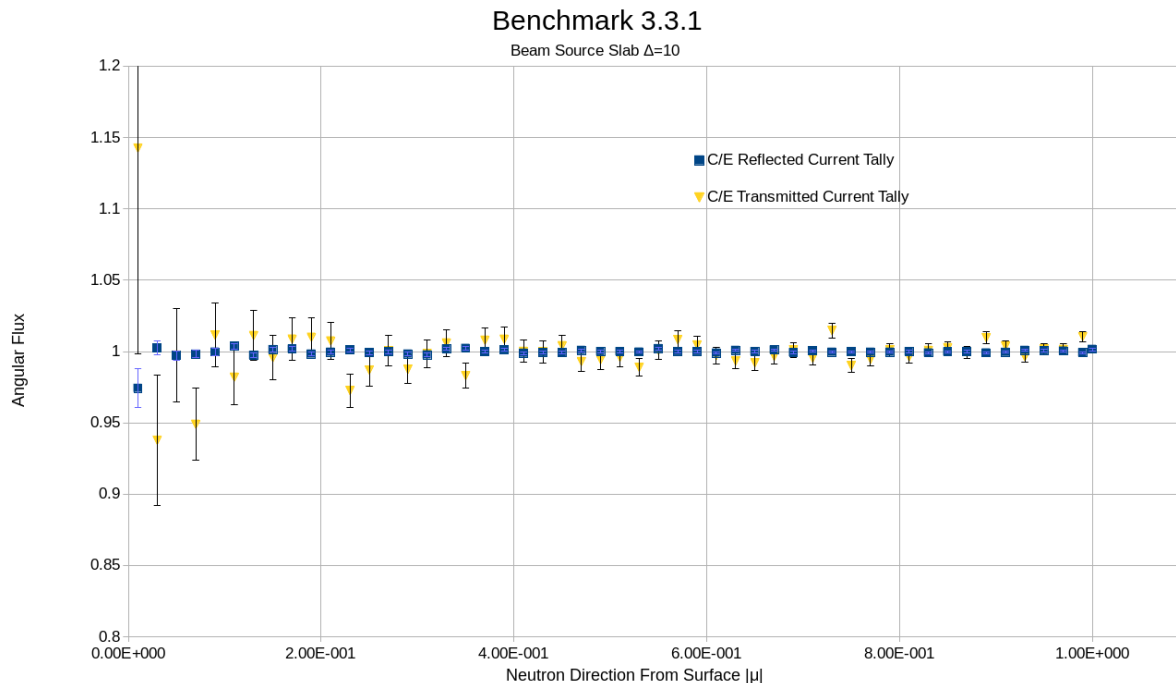


Figure 14: MCNP6 values divided by the analytic solution for Benchmark 3.3.1 ($c=0.9$) for beam source with 10 cm slab.

As can be seen from Figure (14) the reflected tally is much more accurate and precise, while the transmitted tally has more variance. This is most likely because less neutrons make it completely through the slab, since the neutrons have to travel at least 10 mfp to get to the other side. The neutrons also have a higher probability to scatter off the left surface (reflected) thereby improving the statistics on that count.

2.3.2 Benchmark 3.3.1 Beam Source & Varying Slab Thickness (Flux Tally)

The following two cases are exactly the same as the previous two, except that the F2 flux tally was used instead of the F1 current tally.

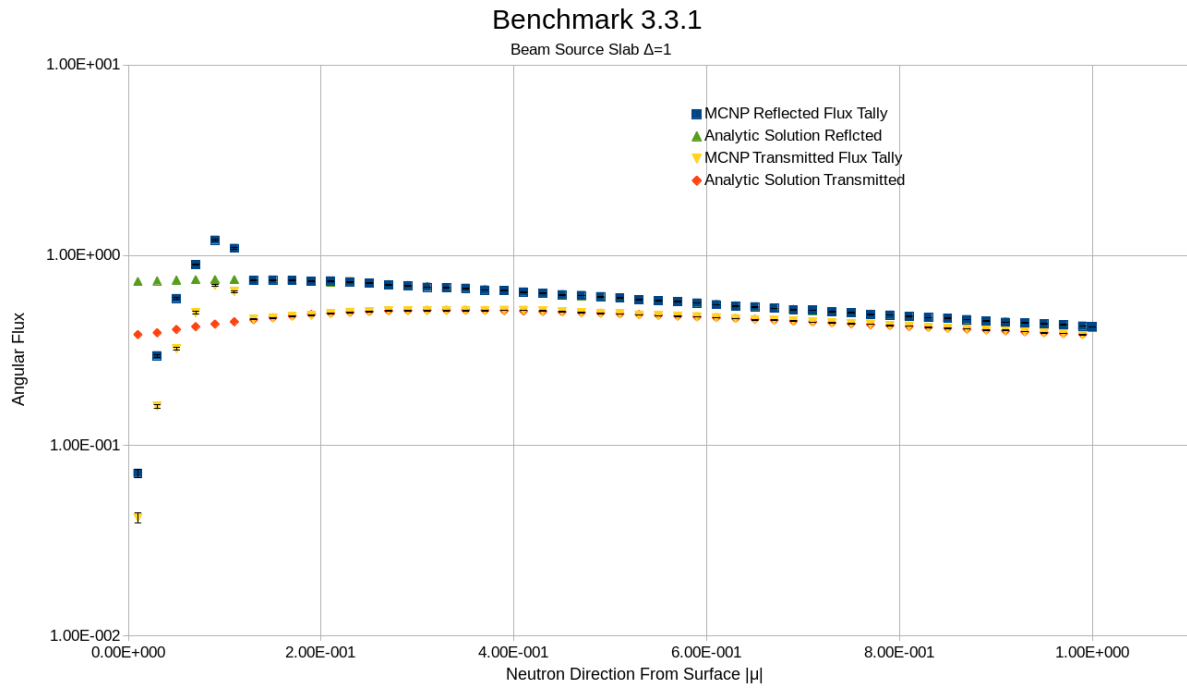


Figure 15: Comparison of analytic results for Benchmark 3.3.1 ($c=0.9$) with MCNP6 results for beam source w/varying slab thickness.

As can be seen in Figure (15) the flux tally distorts the data at low values of μ due to the way the flux tally is tabulated. The rest of the values are very close to the analytic solution, with the percent difference between values being less than 1%.

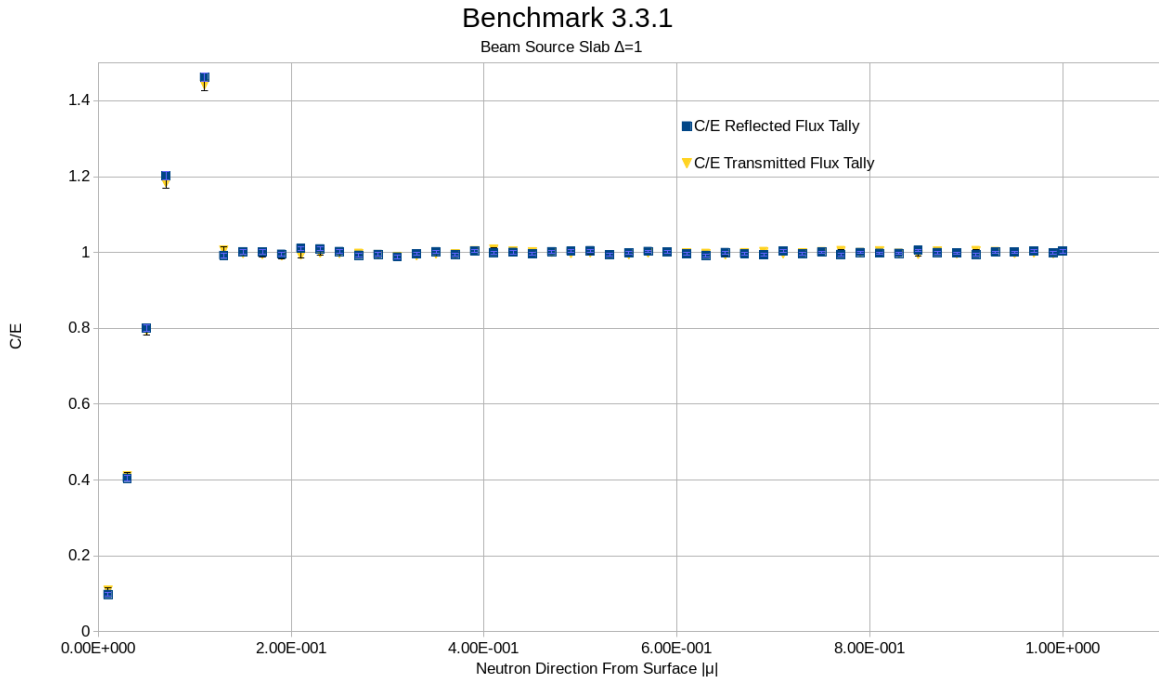


Figure 16: MCNP6 values divided by the analytic solution for Benchmark 3.3.1 ($c=0.9$) for beam source with 1 cm slab.

An interesting note is that for values of $\mu > .1$ the flux tally is more accurate and precise than the current tally for both reflected and transmitted flux.

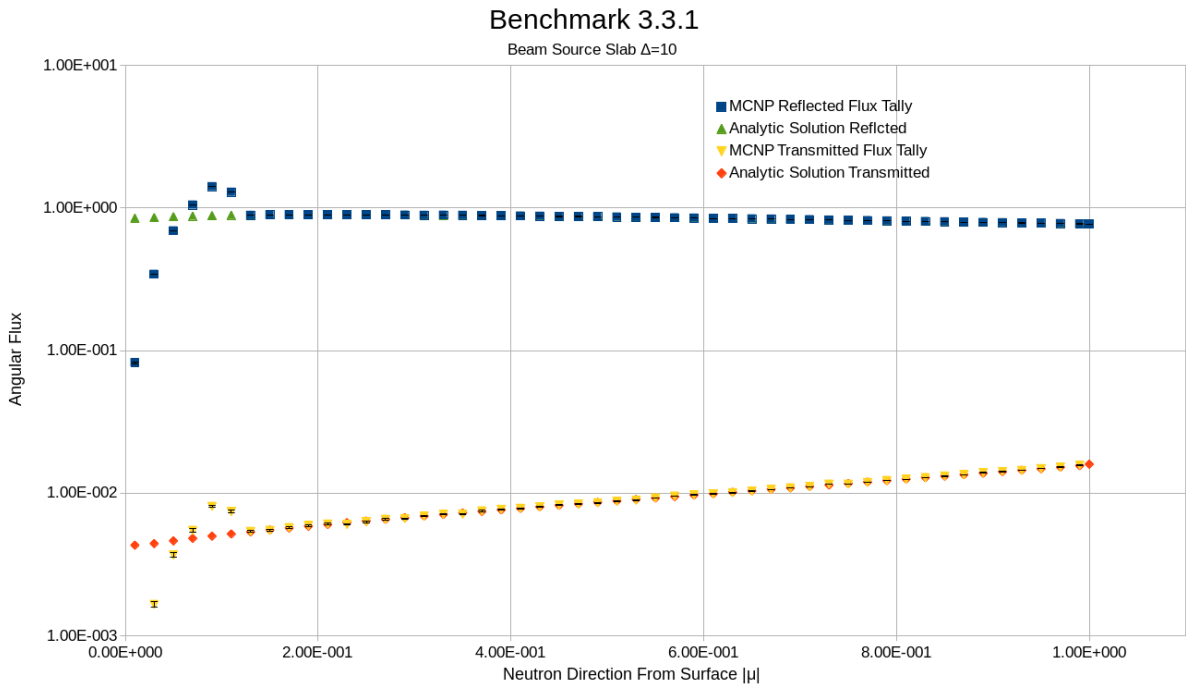


Figure 17: Comparison of analytic results for Benchmark 3.3.1 ($c=0.9$) with MCNP6 results for beam source with 10 cm slab.

The F2 flux approximation at low values of μ is also evident when the slab is 10 cm. The other values match very closely to the analytic values.

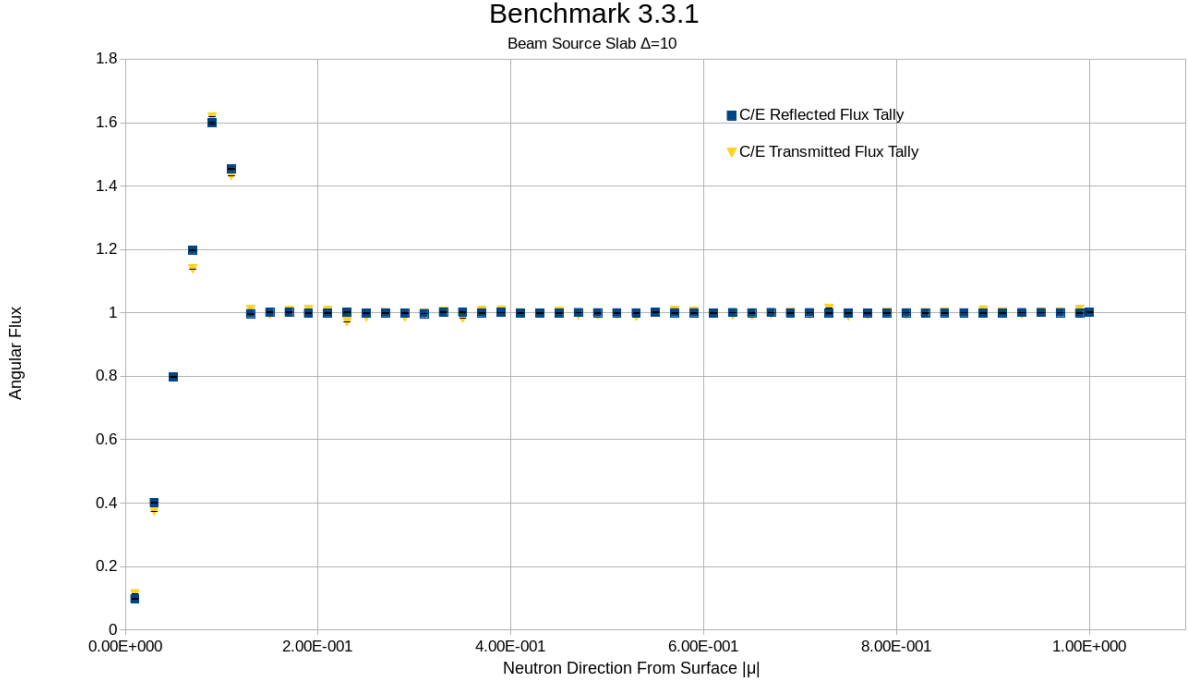


Figure 18: MCNP6 values divided by the analytic solution for Benchmark 3.3.1 ($c=0.9$) for beam source with 10 cm slab.

2.4 Benchmark 3.4

Benchmark 3.4 deals with monoenergetic neutron transport in an isotropically scattering infinite cylinder with a vacuum boundary condition. The equation used to solve this problem is for an isotropically scattering system, without a volume source, and with uniform nuclear properties:

$$[\Omega \cdot \Delta + \Sigma(E)] \phi(r, \Omega, E) = \frac{1}{4\pi} \int_0^\infty dE' \Sigma(E' \rightarrow E) \phi(r, E') \quad (11)$$

where:

$$\Sigma(E' \rightarrow E) \equiv \Sigma_s(E') f_s(E' \rightarrow E) + \nu(E) \Sigma_f(E') \chi(E) \quad (12)$$

In this benchmark as the neutrons enter the outside surface of the cylinder they initiate fission, which leads to the development of a internal flux profile. Professor Ganapol converts this cylindrical transport problem with angular flux boundary conditions into a "pseudo" cylindrical transport problem with an interior source defined. To compare MCNP6 results to the benchmark results reported for the "pseudo" transport problem a volume source must be used over the entire cylinder, with concentric infinite cylinders

bounded by two reflecting surfaces. A flux F2 tally is then defined at each of the concentric cylinders to obtain the MCNP6 results. In his book, professor Ganapol defines a surrogate flux in order to compare the results to other results found in the literature, which is defined as:

$$F(r) = 1 - \frac{\phi(r)}{Q} \quad (13)$$

In order to compare the analytical solution to MCNP6, his results are converted to the "pseudo" flux relative to the external source:

$$\frac{\phi(r)}{Q} = 1 - F(r) \quad (14)$$

2.4.1 Benchmark 3.4.1 Infinite Cylinder with Fission

In this problem the radius of the cylinder is 1 cm, and is infinite along the axis of the cylinder. For the first set of problems the analytic solution matches MCNP6 almost perfectly as can be seen by Figure 19.

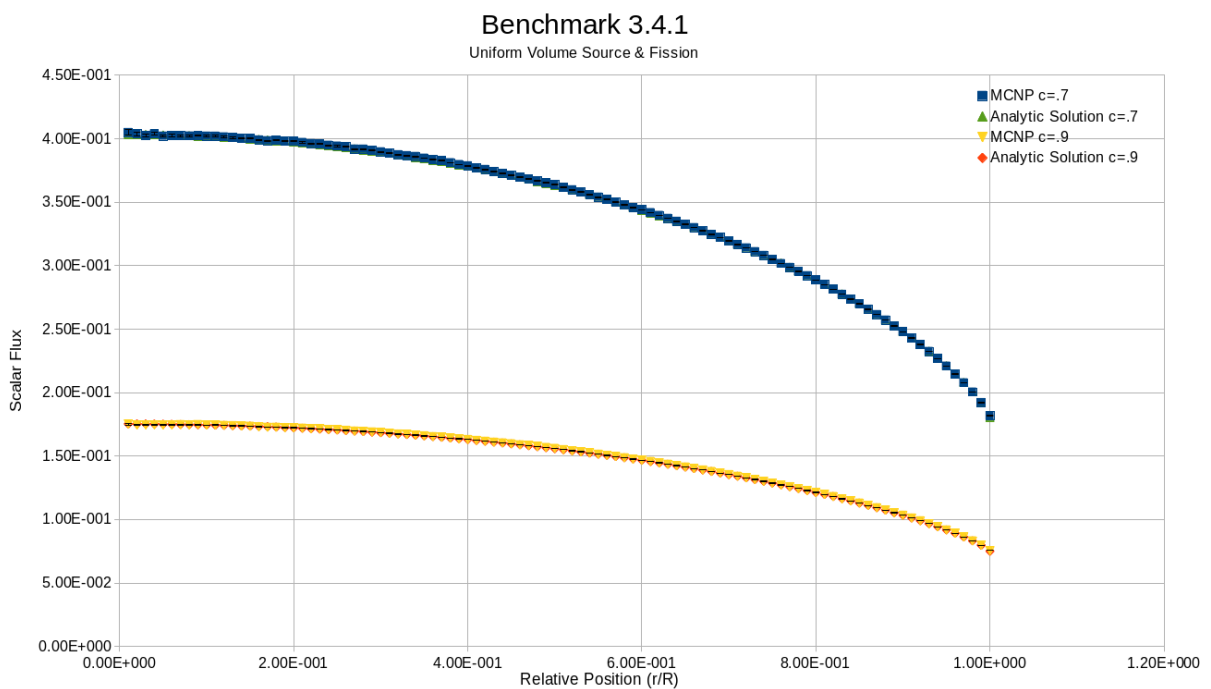


Figure 19: Comparison of the radial flux profile for Benchmark 3.4.1 for two values of c and a radius of 1 cm.

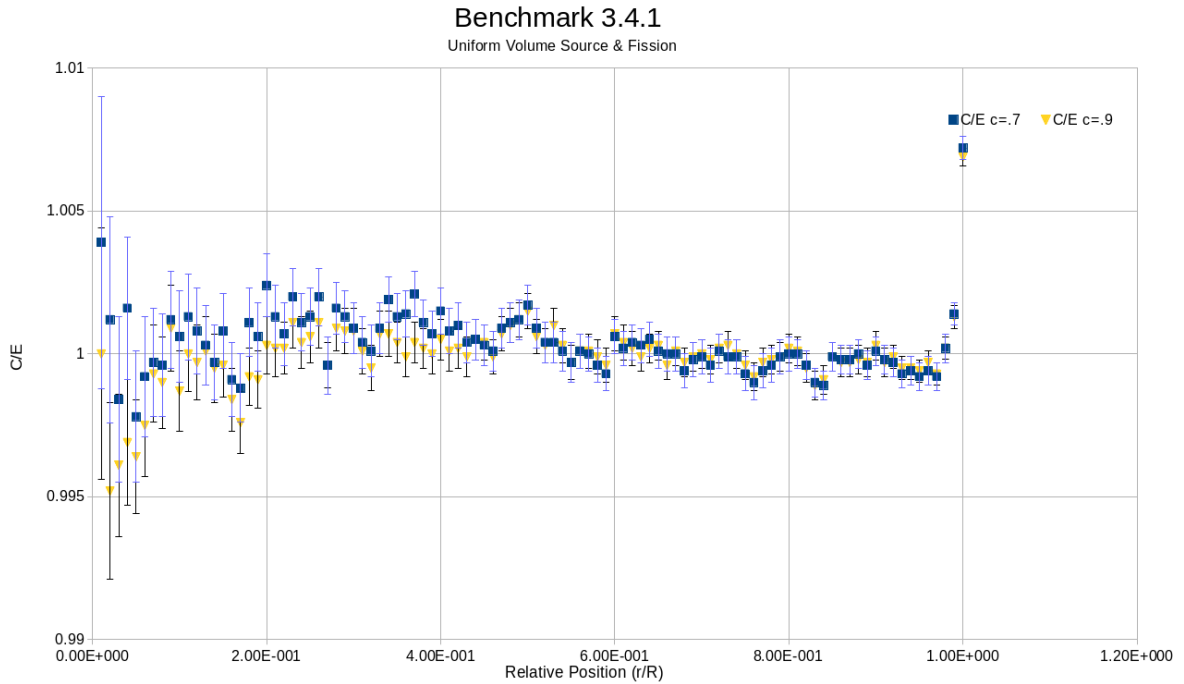


Figure 20: MCNP6 values divided by the analytic solution for Benchmark 3.4.1 for two values of c and a radius of 1 cm.

Most of the results are within statistics, but as you move towards the center of the cylinder the variance increases, most likely due to under-sampling in the region. It can be seen that the flux diverges from the analytic solution at the outside edge of the cylinder. This anomaly is most likely the result of the F2 tally, and low neutron grazing angles relative to the outside surface.

2.4.2 Benchmark 3.4.2 Critical Infinite Cylinder

In his book Professor Ganapol includes a table of values for c and the respective radii for which the infinite cylinder is critical. Two values of c and their respective critical radii were input into a criticality calculation using MCNP6 and compared to the analytical solution, which can be seen in Figure (21). The MCNP6 calculated value of k is within one standard deviation of unity for both cases, and the F2 tally was used to obtain the flux shape.

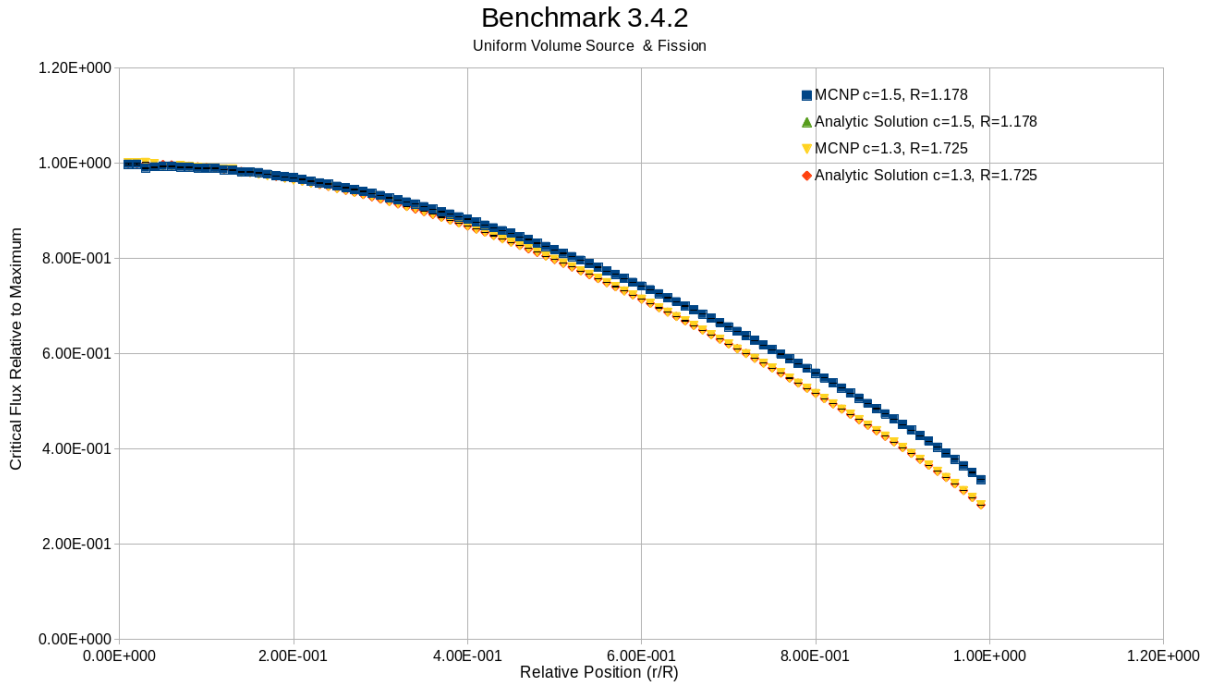


Figure 21: Comparison of the critical flux profile for Benchmark 3.4.2 for two values of c and radii.

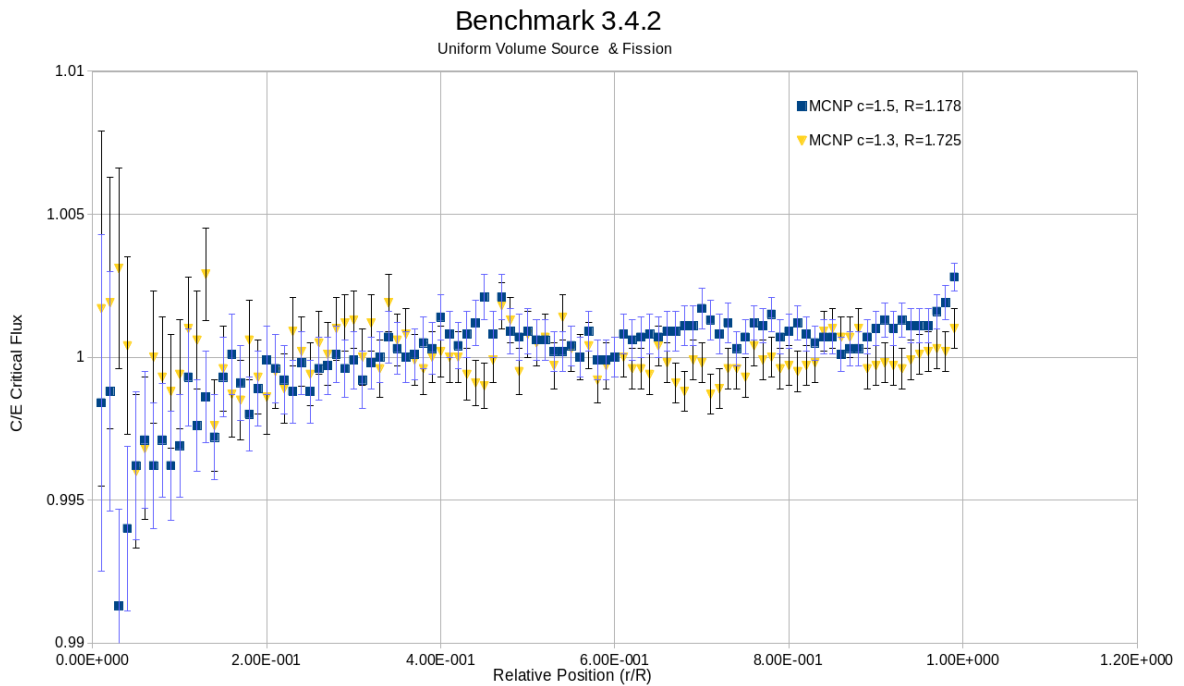


Figure 22: MCNP6 values divided by the analytic solution for Benchmark 3.4.2 for two values of c and radii.

As can be seen from Figure (22), the MCNP6 result diverges from the analytical solution at both the center and outside of the cylinder. This is again most likely due to the F2 tally and neutron grazing angles at the surfaces.

2.5 Comparison between F2 & F4 Tallies

Many of the discrepancies in this benchmark suite are near sources and boundaries, and in order to be sure that the cause is the F2 tally approximation, Benchmark 3.2.2(b) is reworked with the F4 tally.

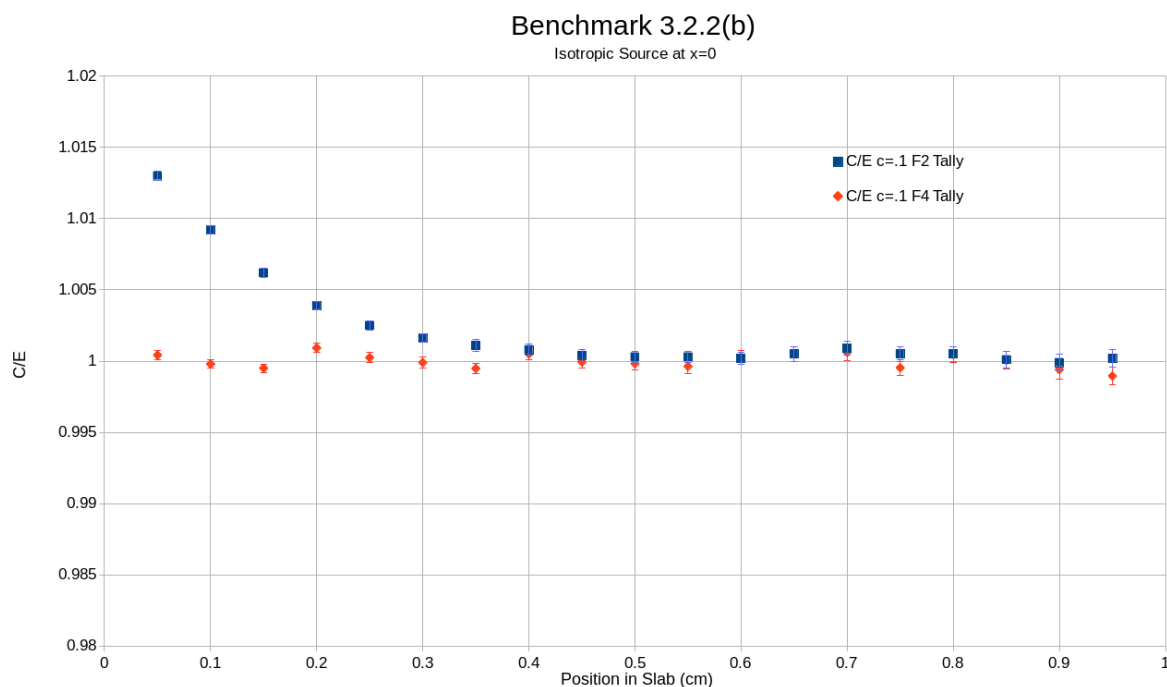


Figure 23: MCNP6 values divided by the analytic solution for Benchmark 3.2.2(b) with the F2 and F4 tally.

As can be seen from Figure (23) the F4 tally does not increase as you approach the source, while the F2 tally increases as has been seen in the other cases. This confirms that that F2 tally is the primary culprit for the divergence of the MCNP6 solution from the analytic answer.

3 Summary

It is extremely important not only to properly set up the source, but to use the correct tallies as well, as can be seen from these cases. The F2 tally can cause issues in high scattering systems, near zones with a high flux gradient, and in systems where neutrons are probable to have low grazing angles with surfaces. To mitigate this discrepancy these problems could be reworked using a F4 volume flux tally

with very narrow volume widths. It is evident that for the most part when the correct source definition and tallies are used, the MCNP6 results match the analytical solution within statistics.

4 Future Work

- Add more benchmarks from Barry Ganapol's book.
- Rework problems using F4 tally.
- Rework the problems using continuous cross-sections rather than multigroup.

5 Acknowledgments

Thank you to Michael Rising, Forrest Brown, and the XCP-3 group at LANL for the help and support. This work was supported by the DOE Nuclear Criticality Safety Program.

References

- [1] Barry Ganapol. *Analytical Benchmarks for Nuclear Engineering Applications - Case Studies in Neutron Transport Theory*. OECD Nuclear Energy Agency, 2008. ISBN: 978-92-64-99056-5.
- [2] MCNP6 Development Team. *Initial MCNP6 Release Overview - MCNP6 version 1.0, Los Alamos National Laboratory, LA-UR-13-22934*. 2013.